

# Theoretical Basis of Higgs-Spin Analysis in $H \rightarrow \gamma\gamma$ and $Z\gamma$ Decays

S.Y. Choi<sup>1</sup>, M.M. Muhlleitner<sup>2</sup>, and P.M. Zerwas<sup>3</sup>

<sup>1</sup> *Department of Physics, Chonbuk National University, Jeonbuk 561-756, Korea*

<sup>2</sup> *Institute of Theoretical Physics, Karlsruhe Institute of Technology, D-76128 Karlsruhe, Germany*

<sup>3</sup> *Deutsches Elektronen-Synchrotron DESY, D-22603 Hamburg, Germany*

(Dated: February 26, 2024)

*We chart the theoretical basis of radiative decays of the Higgs boson,  $H \rightarrow \gamma\gamma$  and  $Z\gamma$ , for measuring the spin of the Higgs particle. These decay channels are complementary to other rare modes such as real/virtual  $Z$ -boson pair-decays. In systematic helicity analyses the angular distribution for zero-spin is confronted with hypothetical spin-2<sup>±</sup> and higher assignments to quantify the sensitivity.*

1. After the discovery of the Higgs particle, the properties must be examined experimentally to identify the particle as the element proper of the Higgs mechanism for breaking the electroweak symmetries [1] [for recent general reviews see Refs.[2]]. The dynamical steps include the confirmation of the scalar spin-zero character of the particle<sup>1</sup>. Higgs-boson decays to pairs of  $Z$ -bosons<sup>2</sup>, cf. Refs.[3–5] and additional references listed there, are promising candidates for examining the Higgs spin at the LHC, supplemented by other measurements in the Higgs-strahlung processes at LHC [6] and  $e^+e^-$  linear colliders [7]. Exploiting the primary Higgs-boson search channels,  $\gamma\gamma$  and  $WW$  decays provide another self-evident tool for spin measurements [8, 9]. [For a variety of methods see the recent literature in Refs.[10]]. All these channels are particularly difficult to analyze for low masses of the Higgs boson where the  $b$ -pair decays are overwhelming. However, with about 126 GeV this is precisely the mass range, where a new boson has been discovered by the LHC experiments [11–13], consistent with analyses of electroweak precision data [14] and compatible with Higgs patterns within the framework of the Standard Model [15].

In this study we examine to which extent radiative decays [16–18]

$$H \rightarrow \gamma\gamma \text{ and } Z\gamma \tag{1.1}$$

can be exploited to determine the spin of the Higgs boson. Even though these decays are rare, with  $BR \simeq 2 \cdot 10^{-3}$  for masses of the order of 126 GeV [19–21], the large number of light Higgs bosons produced in gluon fusion [20–22] generates a sample of order  $10^4$  events in  $\gamma\gamma$  decays for an LHC luminosity of  $\sim 100 \text{ fb}^{-1}$ , and a similar number of  $Z\gamma$ -decay events [though reduced finally by the branching ratio for leptonic  $e, \mu$  decays of the  $Z$ -boson]. These channels nicely supplement the other rare  $ZZ^*$  channels. In the present report we perform general helicity analyses of the radiative decays to quantify the sensitivity to zero-spin of the Higgs boson in angular distributions.

2. The zero-spin character of the Higgs boson reflects itself in the isotropic decay distribution of the radiative decays in the rest frame, i.e.

$$\frac{1}{\Gamma_{\gamma\gamma, Z\gamma}} \frac{d\Gamma_{\gamma\gamma, Z\gamma}}{d\cos\Theta} = 1 \text{ and } 1/2 \tag{1.2}$$

with  $\Theta$  denoting the polar angle of the  $\gamma\gamma$  and  $Z\gamma$  axis, defined, for example, in the Higgs-boson rest frame with regard to the LHC beam axis, Fig.1(a), and with the normalization including the proper statistical factor of the two-photon state. The axis can be reconstructed experimentally in the exclusive  $\gamma\gamma$  and  $Z\gamma$  final states. Since the

<sup>1</sup> This letter expands part of a talk delivered by S.Y. Choi at the APCTP 2012 LHC Physics Workshop at Korea, Seoul, Korea, August 7-9, 2012.

<sup>2</sup> In continuum final states of Higgs-boson decays  $H \rightarrow Z + [f\bar{f}]$  the fermion pair  $[f\bar{f}]$  is not necessarily decay product of a virtual  $Z^*$  state so that general experimental analyses are not constrained by Bose symmetry.

$Z$ -boson is produced in helicity  $\pm 1$  states, the  $\ell\ell$  distribution in leptonic  $Z$  decays is of the familiar  $1 + \cos^2 \theta_\ell$  form,  $\theta_\ell$  being the polar lepton angle in the rest frame of the  $Z$ -boson.

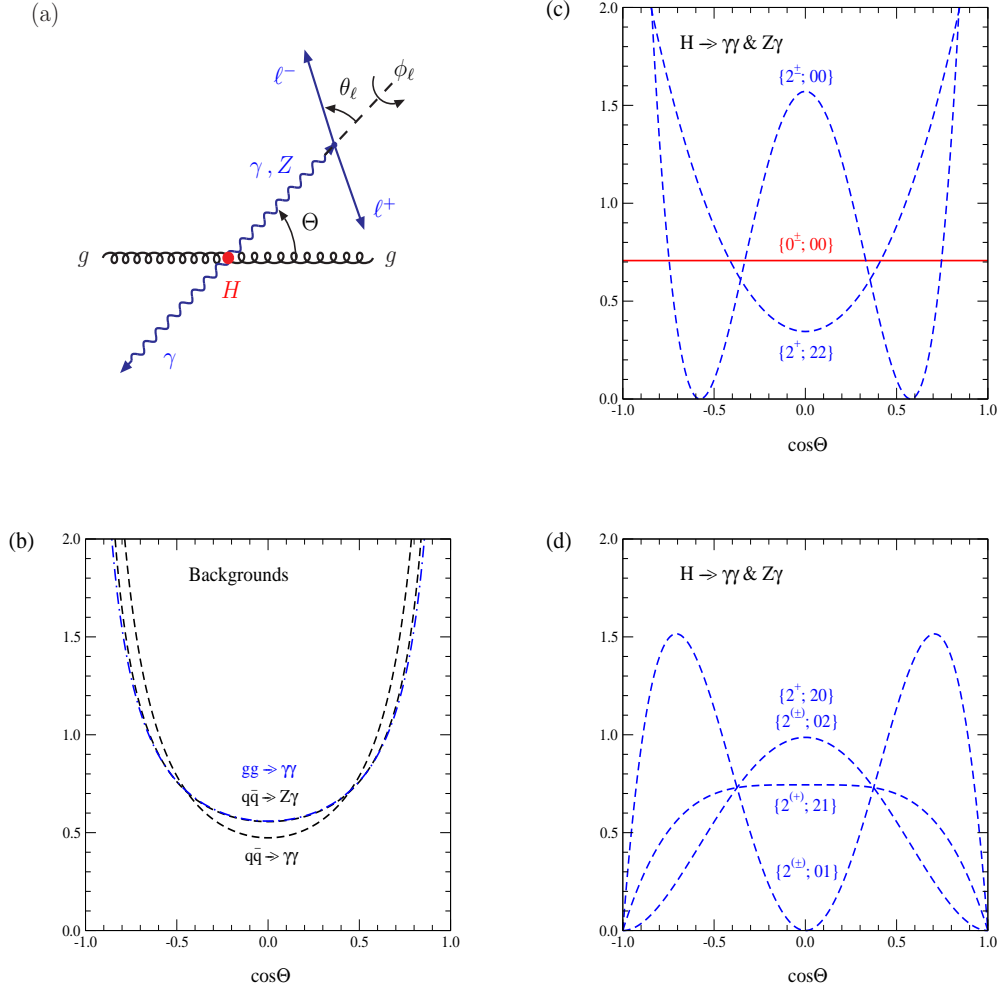


FIG. 1: (a) Kinematics of radiative Higgs-boson decays in gluon fusion; (b-d) Angular distributions of  $\gamma\gamma$  and  $Z\gamma$  axes in the rest frame of the subprocesses: the flat Higgs signal compared with the distributions of the background events with the invariant  $q\bar{q}$  energy set to  $M_H = 126$  GeV in (b) and all potential spin-2 distributions corresponding to the spin component along the collider axis in the rest frame of the Higgs boson, and the difference of the helicities of the vector bosons in the decay final states [all distributions normalized over the interval  $|\cos \Theta| \leq 1/\sqrt{2}$ ]. The upper indices refer to the allowed parity associated with the distributions in  $\gamma\gamma$  decays. Allowed parities of  $Z\gamma$  states are denoted in round brackets either if unique for  $Z\gamma$  or if different from  $\gamma\gamma$  final states. [Note that  $Z\gamma$  states do not conform with the  $gg$  initial states in contrast to  $\gamma\gamma$  states.]

The flat distribution (1.2) is unique to zero-spin of the Higgs boson. For any other spin assignment  $J$  the distribution would be given by the Wigner functions  $\sim |d_{m, \lambda_\gamma - \lambda'_\gamma}^J(\Theta)|^2$  and  $|d_{m, \lambda_Z - \lambda'_\gamma}^J(\Theta)|^2$ , where  $m$  denotes the  $S_z$  spin component being either 0 or  $\pm 2$  for Higgs-boson production in gluon fusion, while  $\lambda_\gamma - \lambda'_\gamma = 0, \pm 2$  and  $\lambda_Z - \lambda'_\gamma = 0, \pm 1, \pm 2$ . The explicit form of the Wigner  $d$ -functions  $d_{m\lambda}^J(\Theta)$  may be read off the tables in Ref. [23].

The general parity-invariant polar angular distribution can be cast into a compact form for any Higgs-spin  $J$  decays

to  $\gamma\gamma$  and  $Z\gamma$  in gluon fusion:

$$\frac{1}{\sigma} \frac{d\sigma[\gamma\gamma]}{d\cos\Theta} = (2J+1) [\mathcal{X}_0^J \mathcal{Y}_0^J \mathcal{D}_{00}^J + \mathcal{X}_0^J \mathcal{Y}_2^J \mathcal{D}_{02}^J + \mathcal{X}_2^J \mathcal{Y}_0^J \mathcal{D}_{20}^J + \mathcal{X}_2^J \mathcal{Y}_2^J \mathcal{D}_{22}^J] \quad (1.3)$$

and

$$\begin{aligned} \frac{1}{\sigma} \frac{d^2\sigma[Z\gamma]}{d\cos\Theta d\cos\theta_\ell} = \frac{3(2J+1)}{16} & \left\{ \left[ \mathcal{X}_0^J \mathcal{Y}'_0^J \mathcal{D}_{00}^J + \mathcal{X}_0^J \mathcal{Y}'_2^J \mathcal{D}_{02}^J + \mathcal{X}_2^J \mathcal{Y}'_0^J \mathcal{D}_{20}^J + \mathcal{X}_2^J \mathcal{Y}'_2^J \mathcal{D}_{22}^J \right] (1 + \cos^2\theta_\ell) \right. \\ & \left. + 2 \left[ \mathcal{X}_0^J \mathcal{Y}'_1^J \mathcal{D}_{01}^J + \mathcal{X}_2^J \mathcal{Y}'_1^J \mathcal{D}_{21}^J \right] \sin^2\theta_\ell \right\} \end{aligned} \quad (1.4)$$

respectively, with the squared Wigner functions  $\mathcal{D}_{m\lambda}^J = \frac{1}{4} \sum [d_{m\lambda}^J(\Theta)]^2$  symmetrized by the summing over all signs  $\pm m, \pm\lambda$  of the spin/helicity components [index 0 counting twice]. The functions read explicitly for  $J=0$  and  $J=2$ :

$$\begin{aligned} \mathcal{D}_{00}^0 &= 1 & \mathcal{D}_{20}^2 &= \mathcal{D}_{02}^2 = 3 \sin^4\Theta/8 \\ \mathcal{D}_{00}^2 &= (3 \cos^2\Theta - 1)^2/4 & \mathcal{D}_{01}^2 &= \mathcal{D}_{10}^2 = 3 \sin^2\Theta \cos^2\Theta/2 \\ \mathcal{D}_{22}^2 &= (\cos^4\Theta + 6 \cos^2\Theta + 1)/16 & \mathcal{D}_{21}^2 &= \mathcal{D}_{12}^2 = \sin^2\Theta(1 + \cos^2\Theta)/4, \end{aligned} \quad (1.5)$$

the functional forms displayed in Fig. 1(c,d). The [non-negative] reduced production and decay helicity probabilities  $\mathcal{X}$  for gluon fusion,  $\mathcal{Y}$  for  $\gamma\gamma$  and  $\mathcal{Y}'$  for  $Z\gamma$  final states, are model-dependent parameters, obeying the sum rules

$$\mathcal{X}_0^J + \mathcal{X}_2^J = 1 \quad (1.6)$$

$$\mathcal{Y}_0^J + \mathcal{Y}_2^J = 1 \quad \text{and} \quad \mathcal{Y}'_0^J + \mathcal{Y}'_1^J + \mathcal{Y}'_2^J = 1. \quad (1.7)$$

[The formalism can easily be transferred to  $q\bar{q}$  production with  $S_z = 0$  or  $\pm 1$  by substituting  $\mathcal{X}_1^J$  for  $\mathcal{X}_2^J$  and  $\mathcal{D}_{1k}^J$  for  $\mathcal{D}_{2k}^J$  ( $k=0,1,2$ ) in the cross sections and in the  $\mathcal{X}$  sum rule. Note however that the rate for signal Higgs production in  $q\bar{q}$  collisions is negligibly small for light quark beams. The initial states  $gg$  and  $q\bar{q}$  mix incoherently in the most general configurations.]

The polar angle of the  $Z$  decay distribution can easily be integrated out, equivalent to the substitutions  $(1 + \cos^2\theta_\ell) \rightarrow 8/3$  and  $\sin^2\theta_\ell \rightarrow 4/3$ . Since the reduced helicity probabilities are non-negative, the coefficients of both the  $(1 + \cos^2\theta_\ell)$  term and the  $\sin^2\theta_\ell$  term inevitably generate non-vanishing maximum/minimum  $\pm \cos^2\Theta$  terms. Thus, observing [in the experimentally ideal case] that the angular distribution is independent of  $\cos\Theta$ , proves unambiguously the spin-zero character of the Higgs particle. At the same time the  $\sin^2\theta_\ell$  term in  $Z\gamma$  final states is predicted to be absent, providing an independent cross-check.

$\mathcal{P} \setminus J$	0	1	2, 4, ...	3, 5, ...
even	1	forbidden	$\mathcal{D}_{00}^J \mathcal{D}_{02}^J$ $\mathcal{D}_{20}^J \mathcal{D}_{22}^J$	$\mathcal{D}_{22}^J$
odd	1	forbidden	$\mathcal{D}_{00}^J$	forbidden

TABLE I: Selection rules for Higgs parity following from observing the polar angular distribution of a spin- $J$  Higgs state in the process  $gg \rightarrow H \rightarrow \gamma\gamma$ .

The observation of spin states in  $gg \rightarrow H \rightarrow \gamma\gamma$  allows [partial] conclusions also on the parity of the states. From Bose symmetry and parity symmetry of the helicity amplitudes  $\mathcal{T}_{\lambda_1\lambda_2}^J = (-1)^J \mathcal{T}_{\lambda_2\lambda_1}^J = \mathcal{P}(-1)^J \mathcal{T}_{-\lambda_1-\lambda_2}^J$ , referring separately to initial and final states [3], the selection rules presented in Tab.I can easily be derived [see also Ref. [24]], complementing global rules noted earlier in the literature. Scalar and pseudoscalar Higgs bosons

cannot be discriminated in the  $\gamma\gamma$  decay mode, neither even/odd parity by observing  $\mathcal{D}_{00}^J$ , and spin correlation effects [7, 25, 26] must be exploited for discrimination. But observing any state with helicity difference  $\Delta\lambda = 2$  in initial or final state determines unambiguously the even-parity character of the Higgs boson. Analogous rules apply also to  $Z\gamma$  final states in gluon fusion and  $\gamma\gamma$  final states in  $q\bar{q}$  annihilation. Either the first or the second index  $\Delta\lambda$  in the  $\mathcal{D}$  functions coming with the production or decay amplitude, respectively, is restricted in parallel to the rules in Tab.I while the respective companion index is unrestricted apart from the standard spin constraints.

The  $\gamma\gamma$  channel is described by two-by-two independent probabilities for production and decay,  $\mathcal{X}_{0,2}^J$  and  $\mathcal{Y}_{0,2}^J$ . Popular choices for experimental simulations are the complementary  $\{J;00\}$  ‘scalar-type’ and the  $\{J;22\}$  ‘tensor-type assignments’:

$$\text{‘scalar-type assignment’} : \mathcal{X}_0^J = \mathcal{Y}_0^J = 1 \text{ and } \mathcal{X}_2^J = \mathcal{Y}_2^J = 0 \quad [J \geq 0] \quad (1.8)$$

$$\text{‘tensor-type assignment’} : \mathcal{X}_0^J = \mathcal{Y}_0^J = 0 \text{ and } \mathcal{X}_2^J = \mathcal{Y}_2^J = 1 \quad [J \geq 2], \quad (1.9)$$

supplemented by the

$$\text{‘mixed-type assignment’} : \mathcal{X}_0^J = \mathcal{Y}_2^J = 0 \text{ and } \mathcal{X}_2^J = \mathcal{Y}_0^J = 1 \quad [J \geq 2] \text{ and ‘1,0’ interchanged, } (1.10)$$

for the signal  $J = 0$  and the hypothetical alternatives  $J \geq 2$ . [The  $\gamma\gamma$  coupling of the tensor-type assignment is equivalent to the KK graviton coupling in  $d = 5$  scenarios [8].] The configurations can be exploited in two ways: (i) One of the two scalar- or tensor-type configurations for  $J \geq 2$  for instance, is sufficient to prove that the spin-zero test of the signal is non-trivial; (ii) However, to prove experimentally that the spin-2 assignment is not realized, the three configurations, which are mutually independent, must necessarily be shown absent. Not observing the double index  $\{J;00\}$ , the state  $\{J^-\}$  is ruled out, while neither observing distributions carrying at least one index 2, the state  $\{J^+\}$  is ruled out, too. Thus any spin  $J \geq 2$  can be rejected for both parities  $\pm$  by angular analyses. – Due to potential longitudinal  $Z$  polarization accounted for by  $\mathcal{Y}_1^J$ , the  $Z\gamma$  final state is described by three independent decay probabilities.

Disregarding  $J = 1$ , as forbidden by the Landau-Yang theorem in  $\gamma\gamma$  decays [24, 27], we will choose  $J = 2$  for illustration. [Part of the distributions have also been noted in Refs. [8, 28].] None of the possible helicity states would generate a flat distribution like spin-zero Higgs-boson decays. It is shown in Fig.1 how the flat signal distribution contrasts with the distributions generated by hypothetical spin  $J = 2$  assignments of both even and odd parity, and the angular distribution of the backgrounds as well [to be analyzed next]. In the final section we will compare the spin-0 distribution, assigned  $J = 0$  and  $m = \lambda_{\gamma,Z} - \lambda'_\gamma = 0$ , specifically with the scalar-type  $\{2;00\}$  and the tensor-type  $\{2;22\}$  distributions, representing the state  $J = 2$  with the two parities  $\pm$ . The  $\{2;00\}$  scalar-type distribution is pronounced in the center like spin-0 after angular cut, and rises in the forward/backward directions like the continuum backgrounds, thus providing a non-trivial analogue to be discriminated experimentally from the Higgs signal. The  $\{2;22\}$  tensor-type distribution rises monotonically to the left and to the right of the center, providing also a valuable discriminant. Both types must be ruled out necessarily to reject experimentally the spin-2 assignment for even and odd parity.

A first global comparison between spin-0 and all the spin-2 distributions is offered by the moments of the polar-angle distributions of the  $\gamma\gamma$  and  $Z\gamma$  event axes<sup>3</sup> noted in Tab.II. The first moments of the spin-2 distributions are characteristically different<sup>4</sup> from the spin-0 distribution and may provide early information on the Higgs spin.

**3.** The large continuum background generated in  $pp(q\bar{q}) \rightarrow \gamma\gamma$  and  $Z\gamma$  processes [and, to a lesser extent, loop-induced gluon fusion] requires stringent cuts in order not to dwarf the signals. The angular characteristics allow to reduce

<sup>3</sup> Angular asymmetries [9] can equivalently be used in global analyses.

<sup>4</sup> The assignments  $\{2;01\}$  and  $\{2;21\}$  can also be discriminated from  $\{0;00\}$  by identifying the  $Z$ -decay angular distributions  $\sin^2 \theta_\ell$  versus  $(1 + \cos^2 \theta_\ell)$ .

	Polar Moments $\langle  \cos \Theta  \rangle / \langle 1 \rangle$	<i>total</i>	<i>cut</i>	<i>Z Decay</i>
$\gamma\gamma, Z\gamma$	spin-0 {0; 00}	1/2	$\sqrt{2}/4$	1
$\gamma\gamma, Z\gamma$	spin-2 {2; 00}	5/8	$5\sqrt{2}/36$	$1 + \cos^2 \theta_\ell$
	{2; 02}	5/16	$35\sqrt{2}/172$	
	{2; 20}	5/16	$35\sqrt{2}/172$	
	{2; 22}	65/96	$155\sqrt{2}/492$	
$Z\gamma$	spin-2 {2; 01}	5/8	$5\sqrt{2}/14$	$\sin^2 \theta_\ell$
	{2; 21}	5/12	$55\sqrt{2}/228$	

TABLE II: Ratios of the first over zeroth moments of the polar angular distributions of the  $\gamma\gamma$  and  $Z\gamma$  axes,  $|\cos \Theta|$ , for zero Higgs spin and for spin 2 of a hypothetical resonance. 'cut' denotes the theoretical cut  $|\cos \Theta| < 1/\sqrt{2}$  on the polar angle of the event axes.

the continuum backgrounds considerably.

The angular distribution of the background events is strongly peaked in the forward and backward directions as a result of the  $t$  and  $u$ -channel exchange mechanisms, in contrast to the flat distribution of the signal. In the rest frame of the parton system, cutting out the singular forward and backward directions  $\Theta \rightarrow 0$  and  $\pi$  [so long as the cross sections are not regularized properly]:

$$\frac{d\sigma}{d\cos\Theta} [q\bar{q} \rightarrow \gamma\gamma] = \frac{2\pi\alpha^2}{3s} Q_q^4 \frac{1}{\sin^2\Theta} [1 + \cos^2\Theta] \quad (1.11)$$

$$\frac{d\sigma}{d\cos\Theta} [q\bar{q} \rightarrow Z\gamma] = \frac{2\pi\alpha^2}{3s} Q_q^2 [v_q^2 + a_q^2] [1 - M_Z^2/s] \frac{1}{\sin^2\Theta} \left[ 1 + \cos^2\Theta + \frac{4M_Z^2 s}{(s - M_Z^2)^2} \right] \quad (1.12)$$

for the invariant parton energy  $\sqrt{s} = M_H$ , electric and weak quark charges denoted by  $Q, v, a$  [29, 30]; the helicity decomposition is familiar from electron-positron collisions, cf. appendix in Ref. [31]. The parton subprocesses are peaked at small angles, regularized by the strong interaction scale  $\Lambda_{QCD}$ . For the given Higgs mass, the angular distribution of  $gg \rightarrow \gamma\gamma$  [32] is surprisingly close to the  $q\bar{q}$  process, cf. Fig. 1(b). Induced by radiative return [33] in  $Z\gamma$ , and self-evident in  $\gamma\gamma$ , the  $\gamma$ 's and the  $Z$ -bosons are traveling primarily along the LHC beam axis. By restricting  $|\cos \Theta|$  to less than  $\cos \Theta_{cut} \leq 1/\sqrt{2}$ , the signal is reduced only modestly, but the background strongly.

4. For illustration of the  $J^P$  sensitivity, we present a set of rough theoretical estimates, rescaled from available experimental data in  $\gamma\gamma$  [11] or based on simulations in  $Z\gamma$  [34]. One photon with transverse energy  $\epsilon_{\text{perp}}$  in excess of 25 GeV was required for  $Z\gamma$  decays, and photons in excess of 40 GeV in  $\gamma\gamma$  decays. Numerically, using  $\cos \Theta = [1 - 4\epsilon_{\text{perp}}^2 M_H^2 / (M_H^2 - M_Z^2)^2]^{\frac{1}{2}}$  and  $[1 - 4\epsilon_{\text{perp}}^2 / M_H^2]^{\frac{1}{2}}$  for the corresponding polar angles in the Higgs rest frame, this is approximately equivalent to the restrictions  $|\cos \Theta| < 0.77$  and  $0.55$ , close to the theoretical cut  $1/\sqrt{2}$  used in the previous section. The  $Z$ -boson was assumed to decay leptonically to  $e, \mu$  pairs.

The error estimates for the  $\gamma\gamma$  final states were performed by rescaling the background event numbers of Ref. [11] in energy, using the theoretical energy dependence of  $q\bar{q} \rightarrow \gamma\gamma$  [ignoring mis-identification from jets in this simplified theoretical estimate], and by raising the luminosity to  $100 \text{ fb}^{-1}$ , leaving us with  $4.6k$  [146k] events after cuts for signal [background], in rough agreement, within a factor two with Ref. [35], after inserting the proper  $K$ -factor. The theoretical angular distribution of the photons in the center range left by the cuts was used as well according to Fig. 1. We have adopted the experimental efficiency of 40% and a resolution of  $\pm 2$  GeV. Experimental refinements such as smearing effects etc. have not been considered in this coarse theoretical picture.

In the same way as Ref. [34] we determined the background event number from the cross section of the  $q\bar{q} \rightarrow Z\gamma$  process which dominates the background compared with  $gg$  collisions and the Drell-Yan process including final-state photon radiation. Similarly to the parameters in Ref. [34] we have adopted the values of 3 GeV for the mass resolution

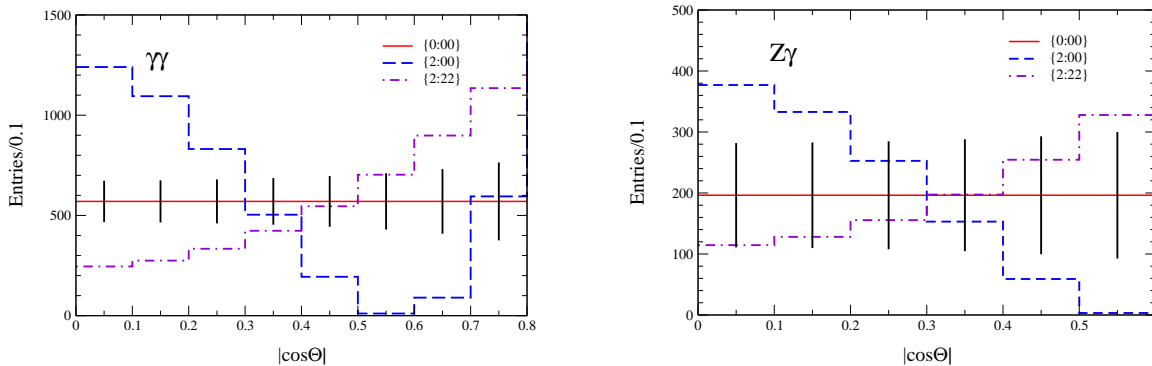


FIG. 2: Left: The angular distribution of the decay axis for spin-0 Higgs-boson decays  $H \rightarrow \gamma\gamma$ ; the spin-0 expectation is compared with the scalar and tensor-type decay distributions of a hypothetical spin-2 particle [theoretical errors only for the LHC luminosity =  $100 \text{ fb}^{-1}$ , event numbers scaled up from [11]]; Right: The same distributions for  $H \rightarrow Z\gamma$  decays [LH-LHC luminosity =  $3 \text{ ab}^{-1}$ ].

and 0.13 for the efficiency<sup>5</sup>. The production cross section of the signal was recalculated theoretically by including the large  $K$ -value in Higgs-boson production  $pp \rightarrow H$ . Finally,  $1.2k$  [51k] signal [background] events were predicted for a luminosity of  $3 \text{ ab}^{-1}$ .

These theoretical estimates of rates and errors, not including detailed experimental refinements, should serve only as a rough illustration of theoretical expectations for Higgs spin analyses in radiative decays.

In the framework defined above, the results for the signals and the size of the roughly expected backgrounds are shown in Fig. 2 for  $H \rightarrow \gamma\gamma$  and  $H \rightarrow Z\gamma$  in the theoretically cut  $\cos \Theta$  range. The solid lines are the [ideal] signals with very high statistics, the error bars, based on the event numbers defined above, represent the theoretical estimates of background fluctuations  $\sqrt{B}$ , contaminating the angular distributions of the signals  $S \ll B$ . These distributions are compared with the expected decay characteristics of a hypothetical spin-2 particle, even/odd parity, derived for the representative angular tensor-type and scalar-type distributions in Eqs. (1.5). Note that the two distributions are mutually complementary to each other. The first  $|\cos \Theta|$  moments [normalized to zeroth moments] are in the ratio  $(0.52 \pm 0.06)/(0.27 \pm 0.05)$  for the tensor/scalar assignment in  $\gamma\gamma$  final states, and  $(0.36 \pm 0.10)/(0.18 \pm 0.08)$  in  $Z\gamma$  final states. Even if added up, the resulting flattish behavior is fractured by the non-zero  $\mathcal{D}_{20} = \mathcal{D}_{02}$  contributions.

The small leptonic  $Z$  branching ratio together with the increased background cross section render experimental  $Z\gamma$  analyses much more demanding than  $\gamma\gamma$  analyses, and a large increase of luminosity is required.

Studying experimentally the  $\gamma\gamma$  and  $Z\gamma$  processes outside the Higgs mass window will yield a good understanding of the background shapes and normalizations. At the expense of a  $\sqrt{2}$  increase of errors one could define a control region with a lower Higgs-type mass window to determine the shapes and use Monte Carlos to extrapolate from the control region to the signal region.

<sup>5</sup> These parameters were extracted by means of PYTHIA [36] and ACERDET [37], with support by D.Zerwas gratefully acknowledged. The transverse momentum of the photon was chosen in excess of 25 GeV. In  $Z$  decays to leptons, electrons or muons were reconstructed with transverse energy/momentum of more than 25 GeV, separated from the photon by  $\Delta R \geq 0.7$ , where  $\Delta R$  is the square-root of the sum of the squares of the azimuthal angle and pseudo-rapidity differences. The invariant mass of the lepton pair was chosen compatible with the mass of the  $Z$  boson within 5 GeV. The reconstructed mass of the Higgs boson was allowed in a window of 3 GeV centered on its nominal mass. The second window can be chosen more restrictive as the Higgs boson width is negligible compared to the experimental resolution, whereas for the  $Z$  boson this is not the case. The resulting efficiency of 0.13 is close to the value reported in Ref. [34] when interpolating slightly different parameters.

**5. Summary:** Dynamical characteristics of the Higgs boson in the Standard Model are particularly difficult to analyze experimentally in the mass region around 126 GeV since the overwhelming decays are  $b$  decays. In this report we have analyzed the theoretical potential of two decay modes,  $H \rightarrow \gamma\gamma$  decays and  $H \rightarrow Z\gamma$  decays [the latter statistically more remote], to measure the spin of the Higgs boson. General helicity analyses prove the sensitivity of both decay modes to zero-spin of the Higgs boson, demonstrated by confronting  $J = 0$  zero-spin for illustration to  $J = 2^\pm$ , i.e. spin = 2 and even/odd parity.

**Acknowledgements.** The work of SYC was supported by Basic Science Research Program through the National Research Foundation (NRF) funded by the Ministry of Education, Science and Technology (2012-0002746). The authors would like to thank M. Schumacher and D. Zerwas for useful experimental support. A correspondence on the selection rules in Table I with S. Weinberg is greatly acknowledged.

- 
- [1] F. Englert and R. Brout, Phys. Rev. Lett. **13** (1964) 321; P. W. Higgs, Phys. Lett. **12** (1964) 132; Phys. Rev. Lett. **13** (1964) 508; Phys. Rev. **145** (1966) 1156. G. S. Guralnik, C. R. Hagen and T. W. B. Kibble, Phys. Rev. Lett. **13** (1964) 585.
  - [2] W. D. Schlatter and P. M. Zerwas, Eur. Phys. J. **H36** (2012) 579 [arXiv:1112.5127 [physics.hist-ph]]; J. Ellis, M. K. Gaillard and D. V. Nanopoulos, arXiv:1201.6045 [hep-ph].
  - [3] S. Y. Choi, D. J. Miller, M. M. Muhlleitner and P. M. Zerwas, Phys. Lett. B **553** (2003) 61 [arXiv:hep-ph/0210077].
  - [4] C. P. Buszello, I. Fleck, P. Marquard and J. J. van der Bij, Eur. Phys. J. C **32** (2004) 209 [arXiv:hep-ph/0212396].
  - [5] K. Hagiwara, Q. Li and K. Mawatari, JHEP **0907** (2009) 101 [arXiv:0905.4314 [hep-ph]]; Y. Gao, A. V. Gritsan, Z. Guo, K. Melnikov, M. Schulze and N. V. Tran, Phys. Rev. D **81** (2010) 075022 [arXiv:1001.3396 [hep-ph]]; A. De Rujula, J. Lykken, M. Pierini, C. Rogan and M. Spiropulu, Phys. Rev. D **82** (2010) 013003 [arXiv:1001.5300 [hep-ph]].
  - [6] J. Ellis, D. S. Hwang, V. Sanz and T. You, arXiv:1208.6002 [hep-ph].
  - [7] V. D. Barger, K. m. Cheung, A. Djouadi, B. A. Kniehl and P. M. Zerwas, Phys. Rev. D **49** (1994) 79 [arXiv:hep-ph/9306270]; D. J. Miller, S. Y. Choi, B. Eberle, M. M. Muhlleitner and P. M. Zerwas, Phys. Lett. B **505** (2001) 149 [arXiv:hep-ph/0102023].
  - [8] J. Ellis and D. S. Hwang, arXiv:1202.6660 [hep-ph].
  - [9] A. Alves, arXiv:1209.1037 [hep-ph].
  - [10] C. Englert, M. Spannowsky and M. Takeuchi, JHEP **1206** (2012) 108 [arXiv:1203.5788 [hep-ph]]; R. Boughezal, T. J. LeCompte and F. Petriello, arXiv:1208.4311 [hep-ph]; D. Stolarski and R. Vega-Morales, arXiv:1208.4840 [hep-ph].
  - [11] G. Aad *et al.* [ATLAS Collaboration], Phys. Lett. B **716** (2012) 1 [arXiv:1207.7214 [hep-ex]]; F. Gianotti, CERN-EP Seminar, July 4, 2012.
  - [12] S. Chatrchyan *et al.* [CMS Collaboration], Phys. Lett. B **716** (2012) 30 [arXiv:1207.7235 [hep-ex]]; J. Incandela, CERN-EP Seminar, July 4, 2012.
  - [13] ATLAS Collaboration, Phys. Lett. B **710** (2012) 383; Phys. Rev. Lett. **108** (2012) 111803; Phys. Lett. B **710** (2012) 49; arXiv:1206.0756 [hep-ex]; arXiv:1206.5971 [hep-ex]; CMS Collaboration, Phys. Lett. B **710** (2012) 91; Phys. Rev. Lett. **108** (2012) 111804; Phys. Lett. B **710** (2012) 284; arXiv:1202.4083 [hep-ex]; CMS-PAS-HIG-12-001; CMS-PAS-HIG-12-007.
  - [14] J. Erler, arXiv:1201.0695 [hep-ph].
  - [15] C. Englert, T. Plehn, M. Rauch, D. Zerwas and P. M. Zerwas, Phys. Lett. B **707** (2012) 512 [arXiv:1112.3007 [hep-ph]]; P. P. Giardino, K. Kannike, M. Raidal and A. Strumia, arXiv:1207.1347 [hep-ph]; J. R. Espinosa, C. Grojean, M. Muhlleitner and M. Trott, JHEP **1205** (2012) 097 [arXiv:1202.3697 [hep-ph]] and arXiv:1207.1717 [hep-ph]; M. Klute, R. Lafaye, T. Plehn, M. Rauch and D. Zerwas, arXiv:1205.2699 [hep-ph]; I. Low, J. Lykken and G. Shaughnessy, arXiv:1207.1093 [hep-ph]; T. Plehn and M. Rauch, arXiv:1207.6108 [hep-ph]; The ATLAS Collaboration, *Coupling properties of the new Higgs-like boson observed with the ATLAS detector at the LHC*, ATLAS-CONF-2012-127.
  - [16] J. R. Ellis, M. K. Gaillard and D. V. Nanopoulos, Nucl. Phys. B **106** (1976) 292; A. Djouadi, M. Spira, J. J. van der Bij



- and P. M. Zerwas, Phys. Lett. B **257** (1991) 187; G. Passarino, C. Sturm and S. Uccirati, Phys. Lett. B **655** (2007) 298 [arXiv:0707.1401 [hep-ph]].
- [17] L. Bergstrom and G. Hulth, Nucl. Phys. B **259** (1985) 137 [Erratum-ibid. B **276** (1986) 744]; A. Djouadi, M. Spira, J. J. van der Bij and P. M. Zerwas, Phys. Lett. B **257** (1991) 187.
- [18] J. S. Gainer, W. Y. Keung, I. Low and P. Schwaller, arXiv:1112.1405 [hep-ph]; A. Freitas and P. Schwaller, JHEP **1101** (2011) 022 [arXiv:1010.2528 [hep-ph]].
- [19] A. Djouadi, J. Kalinowski and M. Spira, Comput. Phys. Commun. **108** (1998) 56 [arXiv:hep-ph/9704448]; A. Djouadi, J. Kalinowski, M. Muhlleitner and M. Spira in J. M. Butterworth et al., [hep-ph/1003.1643].
- [20] M. Gomez-Bock, M. Mondragon, M. Muhlleitner, M. Spira and P. M. Zerwas, arXiv:0712.2419 [hep-ph].
- [21] A. Djouadi, Phys. Rept. **457** (2008) 1 [arXiv:hep-ph/0503172].
- [22] H. M. Georgi, S. L. Glashow, M. E. Machacek and D. V. Nanopoulos, Phys. Rev. Lett. **40** (1978) 692; A. Djouadi, M. Spira and P. M. Zerwas, Phys. Lett. B **264** (1991) 440; S. Dawson, Nucl. Phys. B **359** (1991) 283; R. V. Harlander and W. B. Kilgore, Phys. Rev. Lett. **88** (2002) 201801 [hep-ph/0201206].
- [23] M. E. Rose, Elementary Theory of Angular Momentum, Dover Publications 1995.
- [24] C. N. Yang, Phys. Rev. **77** (1950) 242.
- [25] B. Coleppa, K. Kumar and H. E. Logan, arXiv:1208.2692 [hep-ph].
- [26] T. Plehn, D. L. Rainwater and D. Zeppenfeld, Phys. Rev. Lett. **88** (2002) 051801 [hep-ph/0105325].
- [27] L. D. Landau, Dokl. Akad. Nauk. **60** (1948) 207.
- [28] S. Bolognesi, Y. Gao, A. V. Gritsan, K. Melnikov, M. Schulze, N. V. Tran and A. Whitbeck, arXiv:1208.4018 [hep-ph].
- [29] E. L. Berger, E. Braaten and R. D. Field, Nucl. Phys. B **239** (1984) 52.
- [30] U. Baur, E. W. N. Glover and J. J. van der Bij, Nucl. Phys. B **318** (1989) 106.
- [31] K. Hagiwara, R. D. Peccei, D. Zeppenfeld and K. Hikasa, Nucl. Phys. B **282** (1987) 253.
- [32] Z. Bern, L. J. Dixon and C. Schmidt, Phys. Rev. D **66** (2002) 074018 [hep-ph/0206194].
- [33] M. -S. Chen and P. M. Zerwas, Phys. Rev. D **11** (1975) 58; and Phys. Rev. D **12** (1975) 187.
- [34] S. Kiourkos and J. Schwindling, ATL-PHYS-99-010,  $H^0 \rightarrow Z^0 \gamma$  channel in ATLAS. *A study of the Standard Model and Minimal Supersymmetric SM case.*
- [35] M. Dührssen, ATL-PHYS-2002-030; M. Dührssen *et al* Phys. Rev. D **70**, 113009 (2004); R. Lafaye, T. Plehn, M. Rauch, D. Zerwas and M. Dührssen, JHEP **0908**, 009 (2009),
- [36] T. Sjostrand, S. Mrenna and P. Z. Skands, JHEP **0605** (2006) 026 [hep-ph/0603175].
- [37] E. Richter-Was, hep-ph/0207355.